Original Article | Cardiovascular Imaging

https://doi.org/10.3348/kjr.2018.19.2.247
pISSN 1229-6929 · eISSN 2005-8330
Korean J Radiol 2018;19(2):247-255

Korean Journal of Radiology
KJR

Self-Gated Late Gadolinium Enhancement at 7T to Image Rats with Reperfused Acute Myocardial Infarction

Lei Wang, BD[1]*, Yushu Chen, MD[2]*, Bing Zhang, MD[2], Wei Chen, MD, PhD[2], Chunhua Wang, MD[2], Li Song, BD[1], Ziqian Xu, MD[2], Jie Zheng, PhD[3], Fabao Gao, MD, PhD[2]

[1]Molecular Imaging Center, West China Hospital of Sichuan University, Chengdu 610041, China; [2]Department of Radiology, West China Hospital of Sichuan University, Chengdu 610041, China; [3]Mallinckrodt Institute of Radiology, Washington University School of Medicine in St. Louis, MO 63110, USA

Objective: A failed electrocardiography (ECG)-trigger often leads to a long acquisition time (TA) and deterioration in image quality. The purpose of this study was to evaluate and optimize the technique of self-gated (SG) cardiovascular magnetic resonance (CMR) for cardiac late gadolinium enhancement (LGE) imaging of rats with myocardial infarction/reperfusion.

Materials and Methods: Cardiovascular magnetic resonance images of 10 rats were obtained using SG-LGE or ECG with respiration double-gating (ECG-RESP-gating) method at 7T to compare differences in image interference and TA between the two methods. A variety of flip angles (FA: 10°–80°) and the number of repetitions (NR: 40, 80, 150, and 300) were investigated to determine optimal scan parameters of SG-LGE technique based on image quality score and contrast-to-noise ratio (CNR).

Results: Self-gated late gadolinium enhancement allowed successful scan in 10 (100%) rats. However, only 4 (40%) rats were successfully scanned with the ECG-RESP-gating method. TAs with SG-LGE varied depending on NR used (TA: 41, 82, 154, and 307 seconds, corresponding to NR of 40, 80, 150, and 300, respectively). For the ECG-RESP-gating method, the average TA was 220 seconds. For SG-LGE images, CNR (42.5 ± 5.5, 43.5 ± 7.5, 54 ± 9, 59.5 ± 8.5, 56 ± 13, 54 ± 8, and 41 ± 9) and image quality score (1.85 ± 0.75, 2.20 ± 0.83, 2.85 ± 0.37, 3.85 ± 0.52, 2.8 ± 0.51, 2.45 ± 0.76, and 1.95 ± 0.60) were achieved with different FAs (10°, 15°, 20°, 25°, 30°, 35°, and 40°, respectively). Optimal FAs of 20°–30° and NR of 80 were recommended.

Conclusion: Self-gated technique can improve image quality of LGE without irregular ECG or respiration gating. Therefore, SG-LGE can be used an alternative method of ECG-RESP-gating.

Keywords: *Self-gated; Myocardial infarction; Flip angle; MRI; Late gadolinium enhancement; Animal studies; 7T*

Received February 3, 2017; accepted after revision July 28, 2017.
This work was supported by the National Natural Science Foundation of China (grant number 81520108014, 81528009), and the State's Key Project of Research and Development Plan of China (2016YFA0201402).

*These authors contributed equally to this work.

Corresponding author: Fabao Gao, MD, PhD, Department of Radiology, West China Hospital of Sichuan University, No. 37 Guoxue Alley, Chengdu 610041, China.
• Tel: (8628) 8516 4081 • Fax: (8628) 8542 2135
• E-mail: gaofabao@yahoo.com

INTRODUCTION

Cardiovascular magnetic resonance (CMR) has emerged as a valuable tool for imaging cardiovascular system in small animals due to its non-invasiveness with relatively high spatial resolution and sensitivity of soft tissue contrast for radiation (1). Cine imaging in CMR is used routinely to assess the function of the heart (2, 3). Late gadolinium enhancement (LGE) imaging is now a gold standard for the detection of myocardial infarction (MI) (4). Nevertheless, there are considerable experimental limitations to apply CMR in small animals (5). For example, it is difficult to apply CMR of clinical MRI system to small animals partly

due to their rapid heart and respiratory rates (6). Under anesthesia, heart rates of rats may vary from 400 to 600 beats per minute (7-9) while their respiratory rates may vary from 30 to 60 per minute. External QRS-complex detection device is generally utilized for electrocardiography (ECG) gated CMR (10). However, heart rate depends on respiratory patterns, types of breath-holds (11, 12), and nervous feedback loops (12). Moreover, ECG signal is typically compromised by magneto-hydrodynamic (MHD) effect (i.e., when blood flows through the static magnetic field, it generates electrical fields that can corrupt the measurement of cardiac tissue depolarization) (13). At ultrahigh field like 7T, the susceptibility of ECG recordings to MHD effects is further pronounced (14). Rapid switching of magnetic field gradients with radio frequency (RF) magnetic field pulsing is another factor that can induce electrical fields superimposed on ECG signal (15). Therefore, irregular ECG gating can cause varied repetition time (TR) and affect the recovery of longitudinal magnetization between TR periods (16). This effect is even worse at higher field strengths, resulting in severe cardiac motion artifacts (17).

To address such problem associated with irregular ECG gating, a solution has been proposed and optimized with navigator-based retrospective gating technique called self-gated (SG) imaging approach (18). Navigator signals were acquired along with image data. A trace representative of respiratory motion and cardiac motion can be reconstructed by utilizing changes in MR signal. Navigator signals are retrospectively used to determine cardiac and respiratory cycles, allowing MRI k-space data to be reorganized and reconstructed retrospectively, thus producing cardiac images that are free of motion artifacts without the need for ECG or respiration sensors (3, 19). This technique can eliminate failed-ECG deficits by extracting motion synchronization signal directly from the same MR signal used for image reconstruction. A cardiac and respiratory SG cine CMR has also achieved cine images in small animals without any external ECG or respiration gating (18). Another study has reported that SG method is suitable for cardiac MRI in mice with myocardial infarcts to evaluate infarcted murine heart function (20). However, to the best of our knowledge, no study has assessed SG cine sequence in 7T MRI system to assess myocardial infarct size with LGE imaging. In this work, SG cine CMR techniques were evaluated and optimized to assess MI in a myocardial ischemic/reperfusion rat model commonly having ECG-gating failure (21).

MATERIALS AND METHODS

Animal and Experimental Protocol

The local Institutional Animal Care and Use Committee approved all animal procedures involved in this work. Ten Sprague Dawley rats (males, aged 7–10 weeks) were obtained from Dashuo Animals, Ltd. (Chengdu, China). After being anaesthetized with chloral hydrate (i.p., 0.3 mL/100 g), they underwent surgery to induce MI. The left anterior descending coronary artery was occluded close to its ostium with a snare occluder for 45 minutes. It was then released for reperfusion. Following a visual verification of efficiency of reperfusion, the chest was closed. At 24 hours after the reperfusion, these animals were placed in a 7T MR scanner. Anesthesia was maintained during the whole MR experiment with 1.5% (v/v) isoflurane in oxygen (0.8 L/min) delivered via a nose-cone at a 1 L/min flow rate. Temperature was maintained at 36–37.5°C with a heating pad and monitored using a rectal probe to preserve normothermic conditions during MR experiment. The forelimb and hind-limb of rats were wrapped in a copper foil. Peripheral ECG signal was derived via a silver wire. Core body temperature, ECG, and respiration were monitored with an SAII Model 1030 monitoring and gating system (Small Animal Instruments, Inc., Stony Brook, NY, USA). After acquiring post-MI images, rats were sacrificed for triphenyl tetrazolium chloride (TTC) staining to determine the size of MI.

MRI

All MR acquisitions (Fig. 1) were performed with a 7T system (BRUKER BIOSPEC 70/30, Ettlingen, Germany). A birdcage coil with an inner diameter of 72 mm was used for RF excitation and an array surface coil of 56 mm was used for MR signal reception. Scout imaging was first acquired using gradient-echo sequence to localize short-axis images at the middle level of the left ventricle (LV). For delayed contrast enhancement, 0.6 mmol/kg (1.2 mL/kg) gadobenate dimeglumine was injected via an intravenous route for rats (tail vein) following the initial baseline scanning. All rats were covered with heating pad to keep the temperature stable.

IntraGate fast low angle shot MRI (FLASH), an SG cardiac cine sequence, was used to image LGE in a short-axis view (Fig. 1). Six slices covering the heart from the base to the apex were obtained to evaluate myocardial infarct size after contrast agent was injected. The following sequence parameters were used: TR = 8.0 ms; echo time (TE) = 3.0

Korean Journal of Radiology
KJR

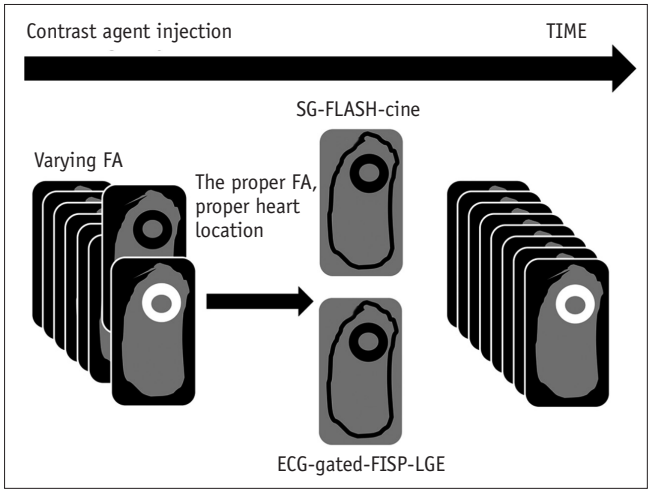

Fig. 1. Schematic summary of MRI protocol. Series of SG images were obtained after gadolinium injection, each with various FA. Last series of images with FAs of 20°–30° were used to select optimal FA images to yield best scar contrast. This FA was then used to perform subsequent SG FLASH imaging between 5–20 minutes after contrast agent administration. FISP-cine-Gate was then obtained following SG-FLASH-cine. ECG = electrocardiography, FA = flip angle, FISP = fast imaging with steady-state precession, FLASH = fast low angle shot MRI, LGE = late gadolinium enhancement, SG = self-gated

ms; flip angles (FAs) = 10°, 15°, 20°, 25°, 30°, 35°, 40°, 60°, 70°, or 80°; field of view (FOV) = 50 x 50 mm; matrix size = 256 x 256; slice thickness = 1.5 mm; and numbers of repetitions (NRs) per slice = 40, 80, 150, or 300. Cine movies with 10 frames per slice were reconstructed retrospectively. Total acquisition times (TAs) varied from 41 to 307 seconds.

As a reference, an ECG-gated fast imaging with steady-state precession (FISP) sequence along with a respiration trigger model was used to acquire LGE images with six slices. Imaging parameters were: TR/TE = 5.1/1.8 ms, FA = 25°, slice thickness = 1.5 mm, FOV = 50 x 50 mm, matrix size = 256 x 256, and the number of signal averages = 2. Total average TA was 220 seconds.

Data Analysis

Two independent observers with five years of experience each in CMR diagnosis who were blinded to imaging parameters and types of sequences visually scored the diagnostic quality of LGE images and delineated the infarcted area. The final infarcted region was defined as the average size measured by two observers. It was expressed as a percentage of the LV. These images were presented to the two observers in a random order. The overall image quality was scored based on a 4-point Likert scale (1 = poor, non-diagnostic; 2 = fair, diagnosis may be impaired; 3 = good, some artifacts but not interfering diagnosis, and good-contrast between normal and infarct myocardium; 4 = excellent, no artifact and excellent-contrast between normal and infarct myocardium). Intra-class coefficient and 95% confidence intervals were calculated to evaluate the concordance between the two types of image scores. A coefficient of 0.7 to 1 indicated good agreement. Infarcted size (%LV) with changed FA and NR were analyzed with one-way analysis of variance (ANOVA). Statistical significance was considered at $p < 0.05$. Quantitative variables are reported as means ± standard deviation (SD). All computations were performed with SPSS version 22 (IBM Corp., Armonk, NY, USA).

Signal intensity in each scar and tissue (SI_scar and SI_tissue) was estimated from the mean value in a region of interest from infarction region and normal myocardium tissues, respectively. Noise was estimated as SD (SD_noise) from a region free of artifact in the background where there was no signal. The equation of contrast-to-noise ratio (CNR) is shown as follows.

CNR = (SI_scar – SI_tissue) / SD_noise

RESULTS

Rats that received surgery were all successfully imaged, revealing enhancement in both SG images and ECG with respiration double-gated images. This was confirmed by TTC staining. Six out of ten rats showed irregular ECG-gating with interferences. SG-LGE images were successfully obtained for all rats free of interferences. Representative short-axial LGE images acquired with SG and ECG-gating are shown in Figure 2. Images with excellent-contrast between normal and infarct myocardium without artifacts could be obtained from ECG-RESP-gating sequence if both ECG and respiration signals are well-triggered (Fig. 2). However, ECG-RESP-gating images suffered from irregular ECG-gating resulting from a large cardiac motion. In contrast, SG scans resulted in artifact-free depiction of MI regardless of the quality of ECG gating (Fig. 2). Size, shape, and location of these MI matched well with those revealed by TTC staining (Fig. 2).

Image Quality

Various FA resulted in different contrast images (Fig. 3). Using FAs of 20°–30°, optimal image contrast was generated between the infarcted myocardium and the remote myocardium. However, when FA was increased up to

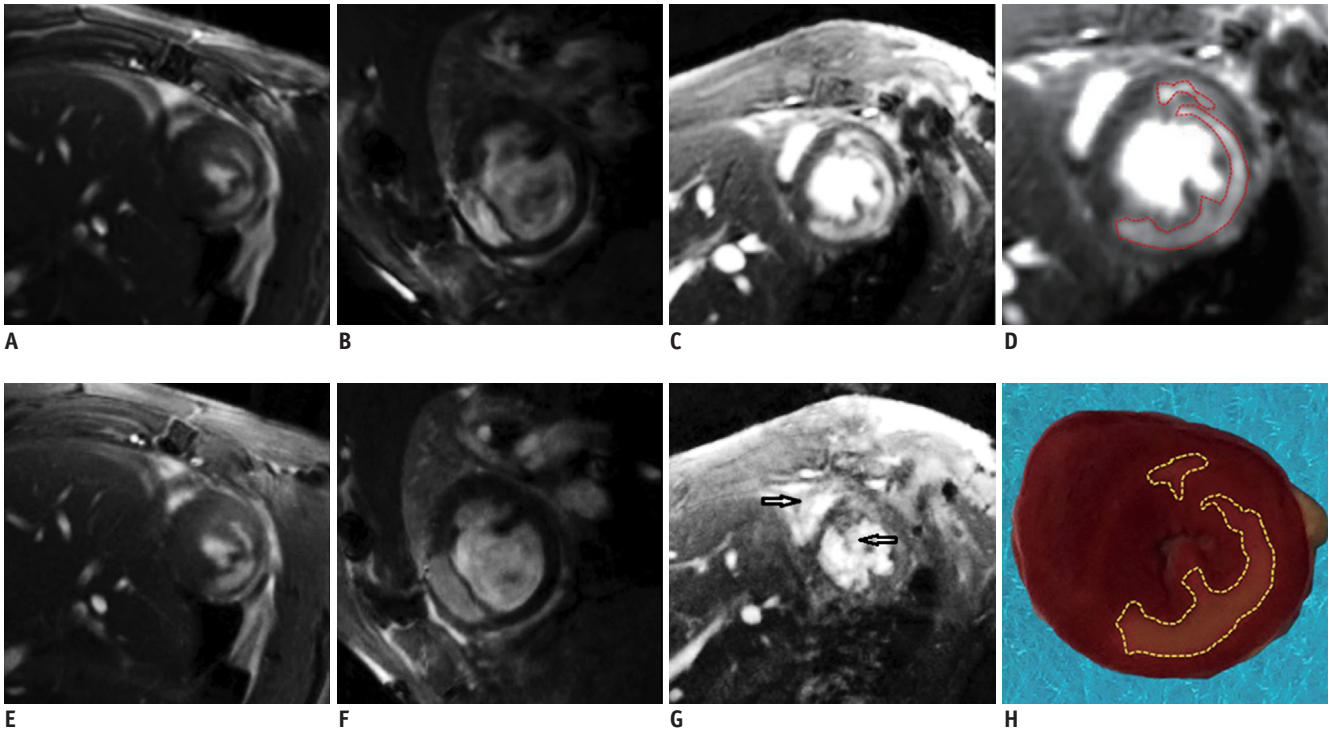

Fig. 2. SG-cine-LGE images (top) and ECG-gated-LGE images (bottom) are shown from three different rats.
(A) and **(E)** are superb images after contrast agent injection whose scores were 4. **(B)** and **(F)** show a few artifacts that would not affect analysis results whose scores were 4. **(C)** and **(G)** were samples that ECG-gated technique could not show good enough images whose score was 1 while good images from SG sequence whose score was 3. **(H)** was triphenyl tetrazolium chloride staining demonstrating that infarction zone (in white or light pink color) was in anterior-lateral, lateral, and posterior-lateral wall of myocardium in **(H)**, in good agreement with SG-LGE in **(D)**. Black arrows **(G)** indicate flow and susceptibility artifacts in ECG-gated image which disappeared in SG image **(C)**.

80°, some anatomic and functional information was lost, such as contrast and boundary in 80% (8/10) of rats (Fig. 3). Moreover, higher FA resulted in more irregular ECG and respiration gating. The image quality score was preferable when FA was at 20°–30° (Fig. 4). Kappa Cohen coefficient was 0.944 (range, 0.917–0.962) in Likert scale obtained from the two observers, indicating an excellent agreement between them. One-way ANOVA revealed no significant differences in infarcted size (%LV) for various FAs ranging from 10° to 40°. When FAs were increased up to 60°–80°, distinguishing the infarcted size (%LV) was difficult sometimes.

One-way ANOVA results showed no significant differences in image scores for different NRs (Table 1). Increasing NR (40, 80, 150, and 300) resulted in increase of TA (41, 82, 154, and 307 seconds, respectively) with the SG-LGE method (Fig. 5). The shortest TA was 41 seconds when NR was set at 40. This was much shorter than the TA when conventional ECG-RESP-gating FISP sequence was used (220 seconds). To reconstruct SG-LGE images with various FAs of 10°–80°, images data were acquired. Only central repetitions without disturbances were utilized, similar to fMRI data reconstruction. Given the relatively large difference in Likert scale score between NR of 80 and NR of 40 (Table 1), optimal NR was recommended to be 80. Since distribution of contrast agent in scar and tissue varied with increasing delay time, both delay time and FAs were critical factors that affected CNRs of SG-LGE images. Due to sequence preparation and TA, it took about 2 minutes to obtain SG-LGE images with varied FAs for each SG scan. FA (bottom x-axis) was 10°, 15°, 20°, 25°, 30°, 35°, and 40°, corresponding to delay time (top x-axis) of 2, 4, 6, 8, 10, 12, and 14 minutes, respectively (Fig. 6). Based on analysis of SG-LGE images, CNR (42.5 ± 5.5, 43.5 ± 7.5, 54 ± 9, 59.5 ± 8.5, 56 ± 13, 54 ± 8, and 41 ± 9) and image quality score (1.85 ± 0.75, 2.20 ± 0.83, 2.85 ± 0.37, 3.85 ± 0.52, 2.8 ± 0.51, 2.45 ± 0.76, and 1.95 ± 0.60) were achieved with different FAs (10°, 15°, 20°, 25°, 30°, 35°, and 40°, respectively).

DISCUSSION

In LGE CMR, an inversion recovery sequence is usually employed to differentiate hyperintensity of infarcted tissue

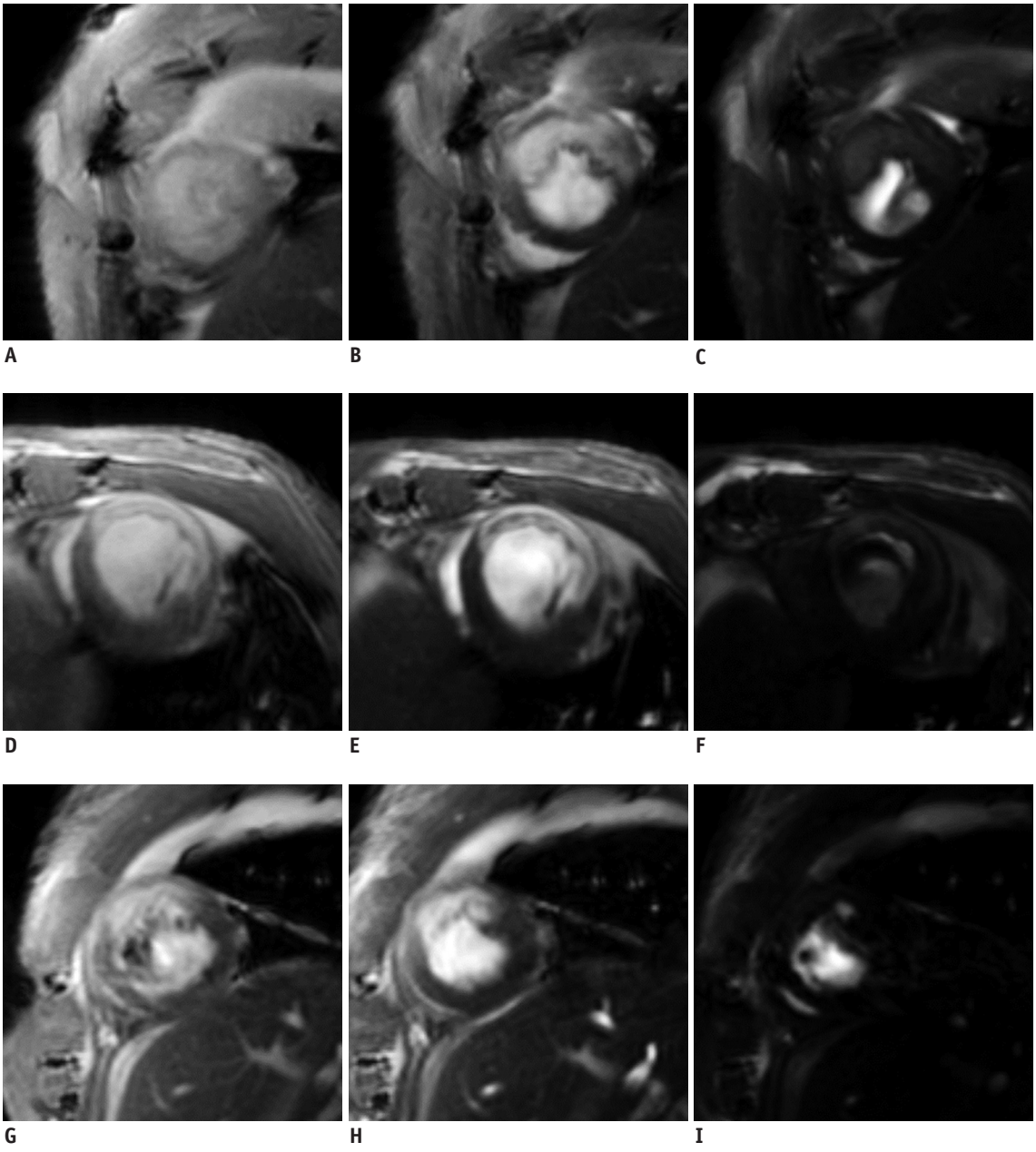

Fig. 3. Varying FA on LGE images are shown for three different rats.
In left column, images **(A, D, G)** had FA of 10°. In middle column, images **(B, E, H)** had FAs of 20°–30°. In right column, images **(C, F, I)** had high FA of 60°–80°.

from the adjacent hypo-intensity of normal tissue (22, 23). Inversion time is adjusted to null normal myocardial signals (24). In other pre-clinical studies, cine LGE CMR represents an attractive alternative to inversion recovery-based LGE CMR for assessing infarct size in mice at high field strengths (7T) (25). Previous studies have evaluated different imaging sequences to assess cardiac function and infarcted size in animal studies (5, 18). Some approaches such as real-time imaging techniques have been developed to avoid failed-ECG gating in images acquisition (26). However, they failed to reveal spatial and temporal resolution provided by segmented acquisition techniques. Several studies have already demonstrated that SG technique can eliminate artifact that irregular ECG-gating technique suffers from (2, 21, 27). Another study has investigated the benefit of motion-based reconstruction for retrospective cardiac cine in small-animal studies using B-spline-based compressed sensing method based on SG sequence (2). It has been suggested that ECG gating can be superseded using SG imaging techniques when cardiac trigger is extracted

directly from MR measurement data (28). To the best of our knowledge, our work is the first effort to investigate the feasibility of using SG technique to detect myocardial infarct size in rat models at 7T MRI. By the method reported in this paper, high quality cine LGE images can be consistently obtained even when ECG-gating fails to trigger correctly inside the cardiac cycle secondary to MI. This study showed that FAs of 20°–30° could be used to create optimal image and contrast between normal and infarcted myocardium tissue. The best FA to obtain optimal contrast depends on each rat condition. In addition, the optimal NR for rats was 80, which was long enough to produce images of quality necessary for diagnostic purposes.

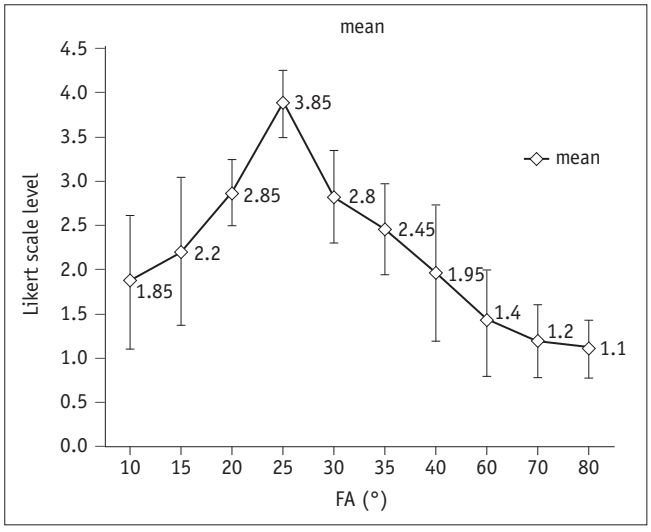

Fig. 4. Likert scale of SG sequence according to FAs. Qualitative grade was higher when FA was 20° to 30°. Qualities were minimized with lower or greater FA.

It is imperative that FA plays an important role in image acquisition. In contrast-enhanced T1-weighted three-dimensional (3D) spoiled gradient-echo sequences, higher FA at 30° can result in optimal contrast between tissue and lesions and improve detection and conspicuity of lesions (29). In cine sequences, T1-weighted image contrast is also strongly affected by sequence parameters TR and FA (30). The signal-to-noise ratio and CNR may be optimized by adjusting the excitation FA (30) when TR is fixed. De Naeyer et al. have confirmed that optimizing FA could increase the reproducibility of kinetic parameter estimates in dynamic contrast-enhanced MRI studies (31, 32). At 1.5T and 3T, optimal excitation angle of 20° for FLASH has been recommended (33). In our research, FAs of 20°–30° are recommended to achieve optimal contrast between infarcted and normal myocardium tissues. This observation is also supported by the following simulation. Based on a previous report on a rat study at 7T (34), the non-contrast myocardial T1 was measured at approximately 1636 msec while the post-contrast normal myocardial T1 was measured at 969 msec. The post-contrast infarction region was measured at 488 msec when 0.2 mmol/kg gadolinium was administered (34). If a 0.6 mmol/kg gadolinium was injected as in our study, assuming a uniform distribution of the contrast media within the rat body and a relaxivity r1 of 3 $msec^{-1}$, the post-contrast normal myocardial T1 would be 488 msec. Because myocardial T1 in the infarction region is

Table 1. One-Way Analysis of Variance Test of Likert Scale Score in Different NR

	NR = 40[a)]	NR = 80[b)]	NR = 150[c)]	NR = 300[d)]	*P**
L (Mean ± SD)	3.21 ± 0.36	3.64 ± 0.44	3.71 ± 0.36	3.79 ± 0.36	> 0.05

**p* values: a) vs. b), 0.093; a) vs. c), 0.254; a) vs. d), 0.254; b) vs. c), 0.564; b) vs. d), 0.564; c) vs. d), 1.0. L = Likert scale score, NR = number of repetitions, SD = standard deviation

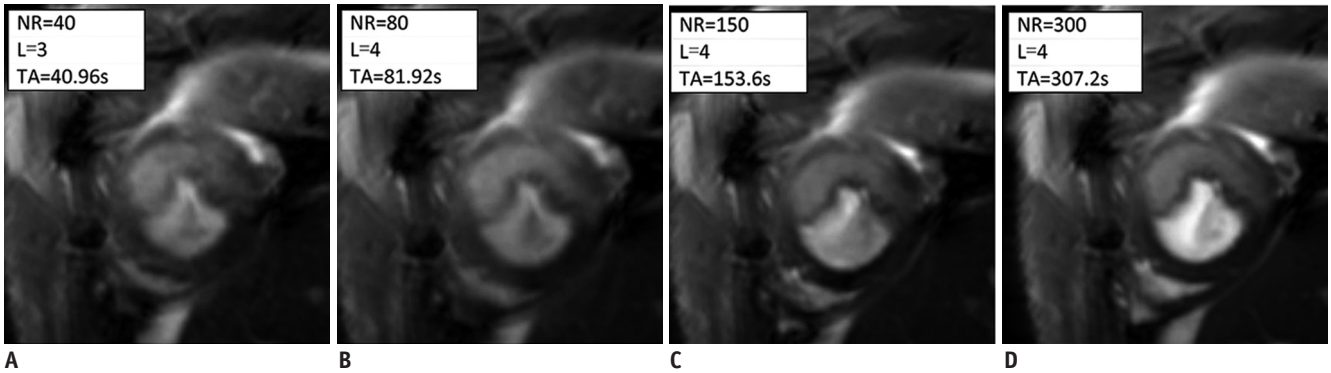

Fig. 5. Image quality and scan time varied with NR. (A-D) had NR of 40, 80, 150, and 300, respectively, with FA of 25°. Scan time was increased with increasing NR. NR = number of repetitions, L = Likert scale score, TA = acquisition time

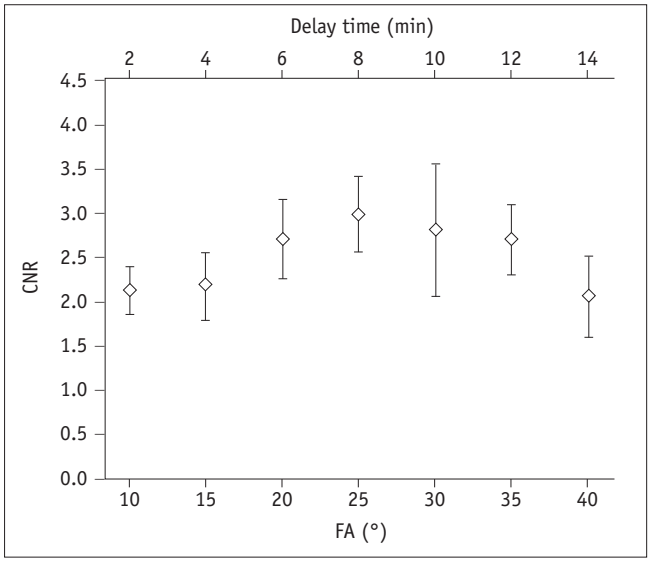

Fig. 6. CNR according to FA and delay time. Both delay time and FA were critical factors that affected CNRs of SG-LGE images. SG-LGE images were acquired within 2 minutes due to sequence preparation and TA for each SG scan. FA (bottom x-axis) was 10°, 15°, 20°, 25°, 30°, 35°, and 40°, corresponding to delay time (top x-axis) of 2, 4, 6, 8, 10, 12, and 14 minutes, respectively. CNR was increased rapidly to maximum values when FAs were 20° to 30° accompanied by delay time of 6 to 10 minutes. CNR = contrast-to-noise ratio

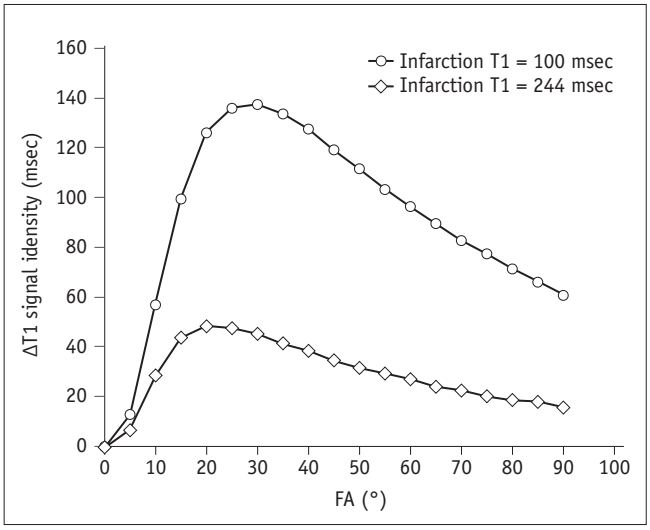

Fig. 7. Simulation of ΔT1 values under various FAs. Vertical axis ΔT1 values refer to deviations of T1 values between normal myocardium and infarction regions. They can be plotted as function of FA. Circle hollow plot: MI T1 = 100 msec; square hollow plot: MI T1 = 244 msec. MI = myocardial infarction

approximately less than half of the normal myocardial tissue (34), we can assume that T1 in the infarction region varies from 100 msec to 244 msec. Based on signal equation of gradient-echo sequences, deviations of T1 values between normal myocardium and infarction regions can be plotted as a function of FA (Fig. 7). The maximal contrast can be achieved with an FA of 20° to 30°, depending on T1 values of infarction regions. Moreover, our study consistently revealed that the maximal quality of contrast could be acquired individually with an FA of 20° to 30° depending on the scanning condition at the time. This means that FA is a vital parameter to obtain an optimal contrast between normal and infarcted myocardium.

Another important advantage of SG sequence is its relatively stable scanning time depending on repetition number rather than ECG-gating condition. NR is used to provide enough scans to extract cardiac and respiratory motion data for the reconstruction of desired cardiac- or respiration cine(s). However, increasing the NR after enough data acquired in SG sequence hardly had any effect on signal contrast, although it affected scan time and image quality associated with motion artifacts. In our study, it took the conventional ECG-gated sequence 3 minutes and 40 seconds to 8 minutes and 25 seconds to image of rats with MI depended on the ECG and respiration signal. With SG-LGE, the recommended 80 repetitions worked well for all rats at different heart rates and respiratory rates. It only spent 1 minute and 21 seconds to acquire the image, which was much less than the traditional FISP sequence.

However, this study has some limitations. It is known that contrast concentration is reduced immediately in coronary artery due to blood circulation once we apply the injection via rat tail vein. This can lead to changes of contrast distribution in myocardium. Besides, previous researches have indicated that contrast is distributed in the extracellular space of normal myocardium but excluded from myocardial cell (35). On the other hand, the contrast medium is distributed in extra- and intracellular spaces after losing myocardial membrane integrity in the infarcted myocardium. For this reason, the infarcted myocardium shows both delayed wash-in and wash-out effects due to distribution in the large extravascular volume compared to normal myocardium. These areas will have higher signal intensities than other areas (35). Contrast distribution in normal myocardium seems to be more sensitive to reduction of contrast concentration in coronary artery during scanning. It might present an accumulated effect in infarcted myocardium. Klein et al (36). have demonstrated that LGE occurs at about 5–30 minutes after contrast application in the infarcted myocardium. Accordingly, we acquired SG-LGE images at 30 minutes after injection and calculated the CNR. We considered that CNRs were mainly influenced by varied FAs and the contrast in both normal

and infarcted myocardium. We also hypothesized that the contrast concentration in the myocardium was related to the delay time. The delay time actually reflected both wash-in and wash-out kinetic effects of contrast distribution in normal and infarcted myocardium as well as the reduction of contrast in coronary artery. According to the equation for CNR calculation, the deviation of signal intensity between the normal and infarcted myocardium in our study was increased rapidly (delay time: 2 to 12 minutes, FAs: 10°–35°) after injection. Contrast might have remained at high level in the infarcted myocardium but reduced in the normal myocardium for the delayed wash-in and wash-out effects in the infarcted myocardium. In this duration, both FA and contrast contributed to the increase of CNR. After 12 minutes (delay time = 12 minutes, FA = 35°), FA may be the primary element that contributed to CNR. However, the recovery of longitudinal relaxation was not enough to generate signal in one TR with large FAs. Therefore, CNR became nearly unreliable. To estimate image quality with varied FAs, using mutable contrast by calculating CNR is unsuitable. In addition, we used the Likert scale of SG sequence to assess qualitative grade of images without calculating CNR with large FAs. Comparative results for infarction size between cine LGE sequence and TTC stains are withheld in the current study. They will be published with other data in the future.

In conclusion, SG cine sequence can acquire LGE images without adverse effects by irregular ECG and respiration gating. Optimal FAs of 20°–30° and NR of 80 are recommended to acquire high quality CMR images within 82 seconds. This finding can help us reliably detect MI in rat models. It will facilitate the evaluation of various treatment options to this important cardiac disease.

REFERENCES

1. Vandsburger MH, Epstein FH. Emerging MRI methods in translational cardiovascular research. *J Cardiovasc Transl Res* 2011;4:477-492
2. Abascal JF, Montesinos P, Marinetto E, Pascau J, Desco M. Comparison of total variation with a motion estimation based compressed sensing approach for self-gated cardiac cine MRI in small animal studies. *PLoS One* 2014;9:e110594
3. Paul J, Divkovic E, Wundrak S, Bernhardt P, Rottbauer W, Neumann H, et al. High-resolution respiratory self-gated golden angle cardiac MRI: comparison of self-gating methods in combination with k-t SPARSE SENSE. *Magn Reson Med* 2015;73:292-298
4. Yang Z, Berr SS, Gilson WD, Toufektsian MC, French BA. Simultaneous evaluation of infarct size and cardiac function in intact mice by contrast-enhanced cardiac magnetic resonance imaging reveals contractile dysfunction in noninfarcted regions early after myocardial infarction. *Circulation* 2004;109:1161-1167
5. Motaal AG, Noorman N, de Graaf WL, Hoerr V, Florack LM, Nicolay K, et al. Functional imaging of murine hearts using accelerated self-gated UTE cine MRI. *Int J Cardiovasc Imaging* 2015;31:83-94
6. Vallée JP, Ivancevic MK, Nguyen D, Morel DR, Jaconi M. Current status of cardiac MRI in small animals. *MAGMA* 2004;17:149-156
7. Berry CJ, Thedens DR, Light-McGroary K, Miller JD, Kutschke W, Zimmerman KA, et al. Effects of deep sedation or general anesthesia on cardiac function in mice undergoing cardiovascular magnetic resonance. *J Cardiovasc Magn Reson* 2009;11:16
8. Constantinides C, Mean R, Janssen BJ. Effects of isoflurane anesthesia on the cardiovascular function of the C57BL/6 mouse. *ILAR J* 2011;52:e21-e31
9. Kramer K, van Acker SA, Voss HP, Grimbergen JA, van der Vijgh WJ, Bast A. Use of telemetry to record electrocardiogram and heart rate in freely moving mice. *J Pharmacol Toxicol Methods* 1993;30:209-215
10. Wang CC, Huang TY. Self-gated PROPELLER-encoded cine cardiac imaging. *Int J Cardiovasc Imaging* 2012;28:1477-1485
11. Berk WA, Shea MJ, Crevey BJ. Bradycardic responses to vagally mediated bedside maneuvers in healthy volunteers. *Am J Med* 1991;90:725-729
12. Kapa S, Venkatachalam KL, Asirvatham SJ. The autonomic nervous system in cardiac electrophysiology: an elegant interaction and emerging concepts. *Cardiol Rev* 2010;18:275-284
13. Dimick RN, Hedlund LW, Herfkens RJ, Fram EK, Utz J. Optimizing electrocardiograph electrode placement for cardiac-gated magnetic resonance imaging. *Invest Radiol* 1987;22:17-22
14. Frauenrath T, Fuchs K, Dieringer MA, Özerdem C, Patel N, Renz W, et al. Detailing the use of magnetohydrodynamic effects for synchronization of MRI with the cardiac cycle: a feasibility study. *J Magn Reson Imaging* 2012;36:364-372
15. Polson MJ, Barker AT, Gardiner S. The effect of rapid rise-time magnetic fields on the ECG of the rat. *Clin Phys Physiol Meas* 1982;3:231-234
16. de Roquefeuil M, Vuissoz PA, Escanyé JM, Felblinger J. Effect of physiological heart rate variability on quantitative T2 measurement with ECG-gated Fast Spin Echo (FSE) sequence and its retrospective correction. *Magn Reson Imaging* 2013;31:1559-1566
17. Fischer A, Weick S, Ritter CO, Beer M, Wirth C, Hebestreit H, et al. SElf-gated Non-Contrast-Enhanced FUnctional Lung imaging (SENCEFUL) using a quasi-random fast low-angle shot (FLASH) sequence and proton MRI. *NMR Biomed* 2014;27:907-917
18. Hiba B, Richard N, Janier M, Croisille P. Cardiac and

respiratory double self-gated cine MRI in the mouse at 7 T. *Magn Reson Med* 2006;55:506-513
19. Crowe ME, Larson AC, Zhang Q, Carr J, White RD, Li D, et al. Automated rectilinear self-gated cardiac cine imaging. *Magn Reson Med* 2004;52:782-788
20. Bovens SM, te Boekhorst BC, den Ouden K, van de Kolk KW, Nauerth A, Nederhoff MG, et al. Evaluation of infarcted murine heart function: comparison of prospectively triggered with self-gated MRI. *NMR Biomed* 2011;24:307-315
21. Hiba B, Richard N, Thibault H, Janier M. Cardiac and respiratory self-gated cine MRI in the mouse: comparison between radial and rectilinear techniques at 7T. *Magn Reson Med* 2007;58:745-753
22. Tham EB, Hung RW, Myers KA, Crawley C, Noga ML. Optimization of myocardial nulling in pediatric cardiac MRI. *Pediatr Radiol* 2012;42:431-439
23. Simonetti OP, Kim RJ, Fieno DS, Hillenbrand HB, Wu E, Bundy JM, et al. An improved MR imaging technique for the visualization of myocardial infarction. *Radiology* 2001;218:215-223
24. Juan LJ, Crean AM, Wintersperger BJ. Late gadolinium enhancement imaging in assessment of myocardial viability: techniques and clinical applications. *Radiol Clin North Am* 2015;53:397-411
25. Protti A, Sirker A, Shah AM, Botnar R. Late gadolinium enhancement of acute myocardial infarction in mice at 7T: cine-FLASH versus inversion recovery. *J Magn Reson Imaging* 2010;32:878-886
26. Brinegar C, Wu YJ, Foley LM, Hitchens TK, Ye Q, Ho C, et al. Real-time cardiac MRI without triggering, gating, or breath holding. *Conf Proc IEEE Eng Med Biol Soc* 2008;2008:3381-3384
27. Ingle RR, Santos JM, Overall WR, McConnell MV, Hu BS, Nishimura DG. Self-gated fat-suppressed cardiac cine MRI. *Magn Reson Med* 2015;73:1764-1774
28. Krämer M, Herrmann KH, Biermann J, Freiburger S, Schwarzer M, Reichenbach JR. Self-gated cardiac Cine MRI of the rat on a clinical 3 T MRI system. *NMR Biomed* 2015;28:162-167
29. Kühn JP, Holmes JH, Brau AC, Iwadate Y, Hernando D, Reeder SB. Navigator flip angle optimization for free-breathing T1-weighted hepatobiliary phase imaging with gadoxetic acid. *J Magn Reson Imaging* 2014;40:1129-1136
30. Busse RF. Flip angle calculation for consistent contrast in spoiled gradient echo imaging. *Magn Reson Med* 2005;53:977-980
31. De Naeyer D, Verhulst J, Ceelen W, Segers P, De Deene Y, Verdonck P. Flip angle optimization for dynamic contrast-enhanced MRI-studies with spoiled gradient echo pulse sequences. *Phys Med Biol* 2011;56:5373-5395
32. Collins DJ, Padhani AR. Dynamic magnetic resonance imaging of tumor perfusion. Approaches and biomedical challenges. *IEEE Eng Med Biol Mag* 2004;23:65-83
33. Tyler DJ, Hudsmith LE, Petersen SE, Francis JM, Weale P, Neubauer S, et al. Cardiac cine MR-imaging at 3T: FLASH vs SSFP. *J Cardiovasc Magn Reson* 2006;8:709-715
34. Zhang H, Ye Q, Zheng J, Schelbert EB, Hitchens TK, Ho C. Improve myocardial T1 measurement in rats with a new regression model: application to myocardial infarction and beyond. *Magn Reson Med* 2014;72:737-748
35. Arheden H, Saeed M, Higgins CB, Gao DW, Bremerich J, Wyttenbach R, et al. Measurement of the distribution volume of gadopentetate dimeglumine at echo-planar MR imaging to quantify myocardial infarction: comparison with 99mTc-DTPA autoradiography in rats. *Radiology* 1999;211:698-708
36. Klein C, Schmal TR, Nekolla SG, Schnackenburg B, Fleck E, Nagel E. Mechanism of late gadolinium enhancement in patients with acute myocardial infarction. *J Cardiovasc Magn Reson* 2007;9:653-658